Ab initio heat capacity and atomic temperature factors of chalcopyrites

H. Neumann
Fritz-Siemon-Strasse 26/111, D-04347 Leipzig, Germany

J. Łażewski,* P. T. Jochym, and K. Parlinski
Institute of Nuclear Physics PAN, Radzikowskiego 152, 31-342 Kraków, Poland

(Received 22 December 2006; revised manuscript received 30 March 2007; published 5 June 2007)

Using first-principles calculations and phonon direct method, thermodynamical properties such as heat capacities and anisotropic and isotropic temperature factors as well as temperature dependence of characteristic Debye temperatures of $AgGaS_2$, $AgGaSe_2$, $AgGaTe_2$, $CuInS_2$, $CuInSe_2$, and $ZnSnP_2$ chalcopyrite compounds have been calculated in harmonic approximation. Obtained results agree quite well with available experimental data taken from literature. From comparison of heat capacities calculated at constant volumes with those measured at constant pressures, we estimate temperature range of harmonic approximation applicability.

DOI: 10.1103/PhysRevB.75.224301 PACS number(s): 63.20.Dj, 31.15.Ar, 62.20.Dc

I. INTRODUCTION

Analyzing critically the experimental lattice vibration data of the ternary chalcopyrite compounds with composition $A^{\mathrm{I}}B^{\mathrm{III}}C^{\mathrm{VI}}$ (A^{I}=Cu, Ag, B^{III}=Al, Ga, In, and C^{VI}=S, Se, Te) and $A^{\mathrm{II}}B^{\mathrm{IV}}C^{\mathrm{V}}$ (A^{II}=Zn, Cd, B^{IV}=Si, Ge, Sn, and C^{V}=P, As) reported in the literature, it has been established that for many of these compounds, there are still considerable discrepancies between the results obtained by different researchers.[1] Recently, it has been shown[2] that in the case of $CuInSe_2$, these discrepancies are essentially caused by deviations from stoichiometry, the resulting formation of various types of crystal defects, and precipitates of secondary phases, and also due to the presence of CuAu-ordered orientation domains in single crystals having nominally the chalcopyrite composition. It is rather likely that the scatter in the lattice dynamics data observed for other $A^{\mathrm{I}}B^{\mathrm{III}}C^{\mathrm{VI}}$ and $A^{\mathrm{II}}B^{\mathrm{IV}}C^{\mathrm{V}}$ semiconductors[1] as well as the discrepancies of experimental results reported for the elastic properties of some of these compounds[3] can be explained in the similar manner. Furthermore, it should be expected that the various types of crystal defects affecting the elastic properties and the lattice vibrations also give rise to thermal properties of the compounds such as the heat capacity or the atomic temperature factors.[4] For instance, it cannot be excluded that highly varying concentration of structural defects or precipitates of secondary phases observed in both compounds[5,6] is the reason for the large differences in the heat capacities measured at elevated temperatures for $AgGaS_2$ (Refs. 7 and 8) and $AgGaSe_2$.[6,9] The very wide scatter in the atomic temperature factors found in structural analysis of $CuInSe_2$ crystals[10,11] could be an indication of the influence of crystal defects on the thermal properties of this compound. In order to assess the reliability of the experimental data on thermal properties of the chalcopyrites and to be able to discuss possible reasons for observed discrepancies, it is plausible to have the heat capacity and the atomic temperature factors of defect-free and stoichiometric crystals of these compounds. Here, we attempt to carry out this task by calculating the thermal properties of some of these compounds on the first-principles basis using the same approach as in our previous studies of zone-center vibrations,[2,12,13] phonon dispersion relations,[14,15] and elastic constants[3] which gave us in all cases good agreement with related experimental data. In addition to the heat capacity and atomic temperature factors, we have also calculated the Debye temperature of the compounds from the elastic constants.

II. THEORETICAL RELATIONS

The first-principles calculations were performed on $2\times2\times1$ supercells with 64 atoms using the VASP package[16] with the plane augmented waves approach[17,18] and gradient corrections.[19,20] The reciprocal space summation was carried out using a $2\times2\times2$ k-point mesh generated according to the Monkhorst-Pack scheme.[21] A plane-wave basis set was limited by a kinetic-energy cutoff varying for considered compounds from 250 to 300 eV. A number of electronic steps were carried out until the total-energy difference in subsequent steps was less than 10^{-8} eV. The ionic step optimization was continued until the residual force components of unconstrained atoms were below 10^{-5} eV/Å. The phonon mode frequencies were calculated using the phonon direct method.[22,23] The complete set of Hellmann-Feynman forces was obtained from small atomic displacements. Using symmetry elements of the $I\bar{4}2d$ space group, the force constants were derived, the dynamical matrix constructed, and finally phonon frequencies were calculated for selected k points in the Brillouin zone (BZ). The phonon densities of states were obtained by sampling the dynamical matrix in 50 000 randomly selected wave vectors in the whole BZ.

In the harmonic approximation, the molar heat capacity at constant volume is given by

$$C_{Vh}(T) = 3nNk_B \int_0^{\omega_m} g(\omega) \frac{(\hbar\omega/k_BT)^2 e^{\hbar\omega/k_BT}}{(e^{\hbar\omega/k_BT}-1)^2} d\omega, \qquad (1)$$

where n is the number of atoms per molecular unit, k_B the Boltzmann constant, $g(\omega)$ the normalized phonon density of states, and ω_m is a maximum phonon frequency. The elements $B_{ij}(\mu)$ of the mean-square displacement tensor of the atom μ were calculated from the corresponding normalized off-diagonal partial phonon density of states $g_{ij,\mu}(\omega)$,[23]

$$g_{ij,\mu}(\omega) = \frac{1}{N}\sum_{l}\int_{\mathrm{BZ}} e_i(\mathbf{k},l;\mu)e_j^*(\mathbf{k},l;\mu)\delta[\omega-\omega(\mathbf{k},l)]d^3k, \tag{2}$$

where $e_i(\mathbf{k},l;\mu)$ is an ith Cartesian component of the polarization vector of the vibration of the μth atom in the lth branch at the $\mathbf{k}$ wave vector. N is a normalization factor. The $B_{ij}(\mu)$ were calculated by means of the relation

$$B_{ij}(\mu) = \frac{\hbar}{2M_\mu}\int_0^\infty g_{ij,\mu}(\omega)\frac{\coth(\hbar\omega/2k_BT)}{\omega}d\omega, \tag{3}$$

where M_μ is the mass of the atom μ. However, for comparison with experimental data, we rendered our results in Debye-Waller exponent form, $\beta_{ij}(\mu)$, using following relation valid in orthogonal unit cells:

$$\beta_{ij}(\mu) = \frac{2\pi^2}{a_i a_j}B_{ij}(\mu), \tag{4}$$

where a_i is the ith lattice constant.

The elastic Debye temperature Θ_D^{el} was calculated by integration over the acoustic wave velocity space with a help of the relation[4]

$$\Theta_D^{el} = \frac{\hbar}{k_B}\left(\frac{9N}{V}\right)^{1/3}\left[\int_\Omega\left(\frac{1}{V_i^3}+\frac{1}{V_j^3}+\frac{1}{V_k^3}\right)d\Omega\right]^{-1/3}. \tag{5}$$

The velocities V_i, V_j, and V_k were calculated from the eigenvalues of the Christoffel equations,

$$(L_{ik}-\varrho V^2\delta_{ik})U_k = 0, \quad i,k = 1,2,3, \tag{6}$$

with the matrix elements

$$\begin{aligned}
L_{11} &= n_1^2c_{11}+n_2^2c_{66}+n_3^2c_{44},\\
L_{22} &= n_1^2c_{66}+n_2^2c_{11}+n_3^2c_{44},\\
L_{33} &= n_1^2c_{44}+n_2^2c_{44}+n_3^2c_{33},\\
L_{12} &= n_1n_2(c_{12}+c_{66}),\\
L_{13} &= n_1n_3(c_{13}+c_{44}),\\
L_{23} &= n_2n_3(c_{13}+c_{44}).
\end{aligned} \tag{7}$$

Here, the U_k are the direction cosines of the particle displacements, the n_i are the components of the unit vector in the considered wave propagation direction, the c_{ij} are the elastic stiffness constants, and ϱ is the mass density of the compound. The elastic stiffness constants for each material were obtained from calculated stress-strain relations for a deformed crystal by the singular value decomposition.[24] The above procedure has some advantages as well as disadvantages with respect to rigorous Brillouin-zone integration. The main advantage is good accuracy of calculation in important area close to the gamma point, which is usually poorly represented in the calculated phonon data. This key area is very well reproduced by elastic data.

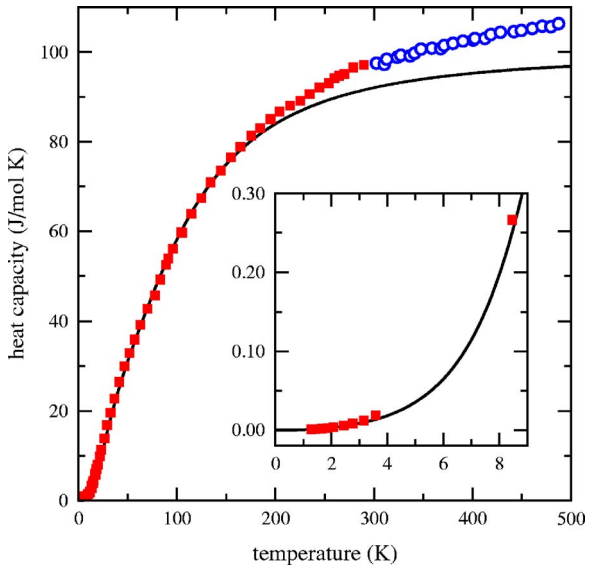

FIG. 1. (Color online) Calculated (solid line) heat capacity of $CuInS_2$. The experimental data are taken from Ref. 30 (filled squares) and Ref. 31 (open circles). Inset: low-temperature range.

III. RESULTS AND DISCUSSION

A. Heat capacity and Debye temperature

In order to demonstrate the accuracy achieved in the first-principles heat capacity calculations, we first compare theoretical results of C_{Vh} taken from Eq. (1) and experimental data of $CuInS_2$ for the following two reasons. Firstly, it follows from infrared reflectivity,[25,26] infrared absorption,[25,27] and Raman scattering measurements[25,28] on bulk single crystals that, in contrast to the situation observed in many other chalcopyrite compounds,[1] the zone-center vibrational mode frequencies are always the same independent of the growth method used to produce the crystals or postgrowth treatments. Therefore, it is plausible to assume that in this compound, the tendency to deviate from stoichiometry or to form sufficiently high concentration of structural defects affecting the lattice vibration spectrum is only weakly pronounced. The same conclusion follows from the phase diagram studies[29] in the system Cu_2S-In_2S_3. Secondly, the isobaric heat capacity $C_p(T)$ of $CuInS_2$ has been measured for temperatures from 1 to 500 K.[30,31] This allows for a comparison of theory and experiment over a wide temperature range. In Fig. 1 the isochoric heat capacity $C_{Vh}(T)$ for $CuInS_2$ calculated in the harmonic approximation with application of Eq. (1) is compared with the measured isobaric heat capacity $C_p(T)$. The inset in Fig. 1 for the temperature range below 10 K shows that the theoretical values tend slightly to underestimate the experimental heat capacity but this difference remains small. The discrepancy remains $C_p - C_{Vh} < 1.5$ J/mol K up to about 100 K, which in this temperature range is within an error limits of the experimental measurements.[30] This result indicates that the contribution of lattice anharmonicity to the heat capacity is very small and can be neglected at $T \leqslant 100$ K which agrees with the observed rapid decrease of the thermal-expansion coefficients of the compound at temperatures below 200 K.[32] The con-

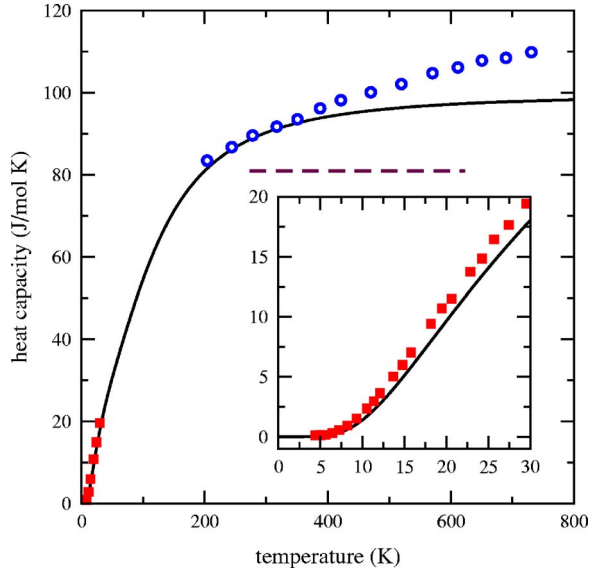

FIG. 2. (Color online) Comparison of heat capacity calculated for $AgGaS_2$ with experimental data taken from Ref. 30 (filled squares), Ref. 7 (open circles), and Ref. 8 (dashed line). Inset: low-temperature range.

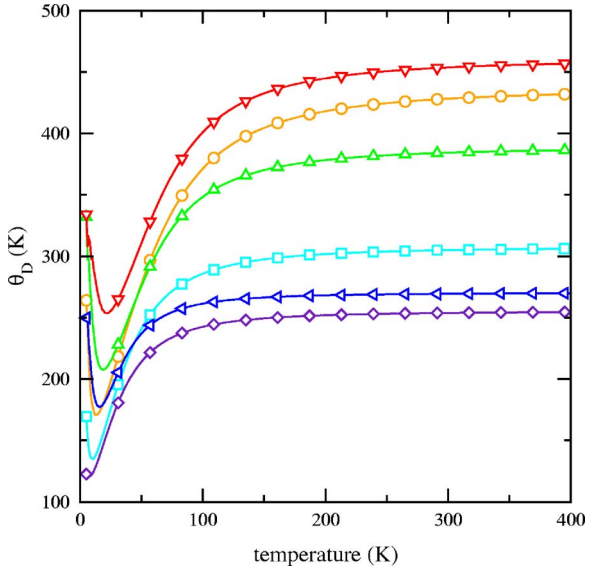

FIG. 4. (Color online) Calculated elastic Debye temperatures for $AgGaS_2$ (circles), $AgGaSe_2$ (squares), $AgGaTe_2$ (diamonds), $CuInS_2$ (up triangles), $CuInSe_2$ (left triangles), and $ZnSnP_2$ (down triangles).

tinuously increasing difference $C_p - C_{Vh}$ at higher temperatures (Fig. 1) up to about $C_p - C_{Vh} = 12$ J/mol K at 500 K can be explained by the influence of lattice anharmonicity which leads to thermal expansion and consequently to additional contribution to the heat capacity. The influence of defects on the C_{Vh} cannot be easily separated from other effects, such as anharmonicity, but one should expect that it is small in low temperatures where there is not enough energy in the system for new defect formation. Existing defects may only contribute very little to the C_{Vh} since they do not have very strong influence on the phonon density of states distribution.

Based on the results for $CuInS_2$, it can be expected that the isochoric heat capacity C_{Vh} of the $AgGaX_2$ compounds (X=S, Se, Te) calculated on a first-principles basis should also agree with measured isobaric heat capacities C_p at sufficiently low temperatures ($T < 100$ K) where lattice anharmonicity effects are still negligible, because these compounds show the same trends of temperature dependence of their thermal-expansion coefficients.[33,34] Unfortunately, related experimental data are scarce and limited to measurements in the temperature range from 1.2 to 40 K for $AgGaS_2$ by Abrahams and Hsu[35] and for temperatures from 1 to 5 K for $AgGaTe_2$ by Bachmann *et al.*[30] To our best knowledge, no low-temperature experimental heat capacity data have been reported for $AgGaSe_2$.

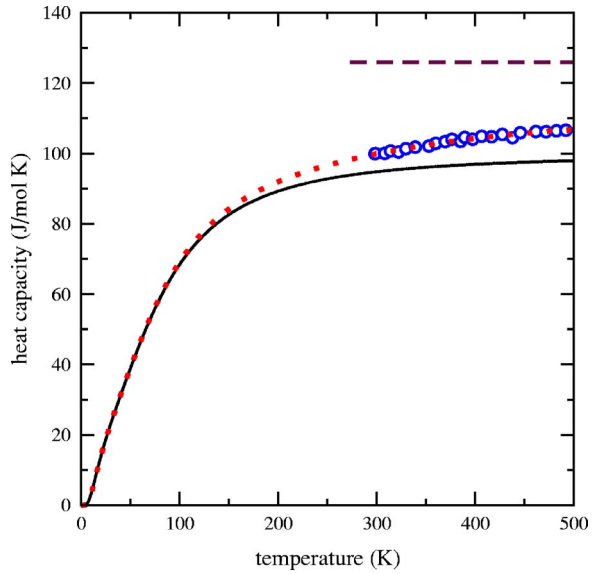

FIG. 3. (Color online) Comparison of experimental [open circles (Ref. 9) and dashed line (Ref. 8)] C_p of $AgGaSe_2$ with calculated C_{Vh} (solid line) and fitted C_p (dotted line) using relation (8).

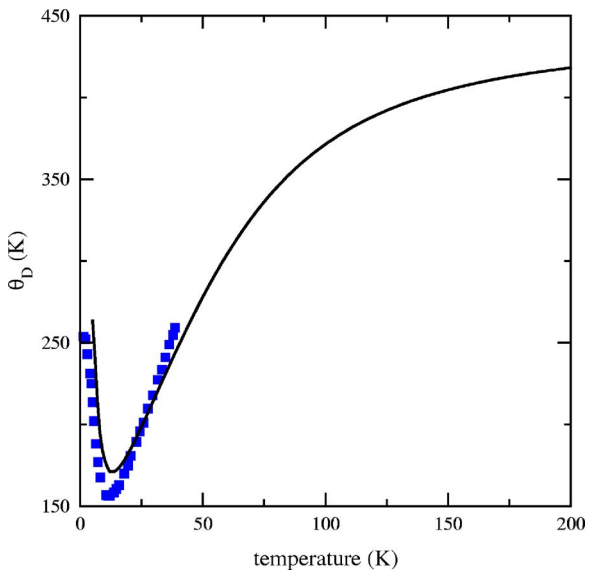

FIG. 5. (Color online) Temperature dependence of elastic Debye temperature of $AgGaS_2$. Experimental data (filled squares) are taken from Ref. 30.

A comparison between theory and experiment of the low-temperature heat capacities of $AgGaS_2$ is shown in the inset of Fig. 2. In analogy to the results for $CuInS_2$ (Fig. 1), we find again the tendency of C_{Vh} to slightly underestimate the true heat capacity, but the difference $C_p - C_{Vh}$ is of the same order of magnitude in both compounds. In both cases, these deviations remain within the error limits of the heat-capacity measurements.[30,35] For temperatures above 200 K, experimental isobaric heat capacities of $AgGaS_2$ have been reported by Neumann and Nowak[7] for the range $T=200-750$ K and by Brisson *et al.*[8] for $T=273-623$ K. For $AgGaSe_2$, experimental values of C_p have been published by Neumann *et al.*[9] for $T=300-500$ K and by Brisson *et al.*[8] for $T=273-673$ K. A comparison of these results with the calculated isochoric heat capacities is presented in Fig. 2 for $AgGaS_2$ and Fig. 3 for $AgGaSe_2$. An increasing difference $C_p - C_{Vh}$ is noticed at higher temperatures.[36] This difference for the low-T regime can be expanded to the Taylor series,

$$\Delta C_p(T) = C_{Vh}(T)(c_1 T + c_2 T^2 + c_3 T^3 + \cdots). \quad (8)$$

The c_1 coefficient is related to the volume expansion coefficient (α_V) in the low-temperature regime by the relation

$$C_{Vh} c_1 = \alpha_V^2 B_T V, \quad (9)$$

where V is a volume and B_T the isothermal bulk modulus. c_2 and c_3 do not have simple physical meaning but allow us to estimate the temperature where the $c_2 T^2$ term starts to play significant role and the accuracy of the harmonic approximation decreases. In the case of $AgGaSe_2$ (dotted line on Fig. 3), expansion coefficients reach following values $c_1 = 3.20 \times 10^{-5}$ K^{-1}, $c_2 = 7.83 \times 10^{-7}$ K^{-2}, and $c_3 = -9.69 \times 10^{-10}$ K^{-3}. For these values, derived heat-capacity relative difference $(C_p - C_{Vh})/C_{Vh}$ reaches 5% level at $T=284$ K.

Starting from the already reported[3] data for $AgGaX_2$ and $CuInX_2$ as well as new elastic data calculated for $AgGaTe_2$ and $ZnSnP_2$, we have calculated the elastic Debye temperatures with Eq. (5). The results are shown in Fig. 4. The range of resulting elastic Debye temperatures is fairly large—the difference between the smallest and the largest is of a factor of ≈ 2. Unfortunately, we were unable to find any experimental data for most of the compounds, except for a low-temperature data for $AgGaS_2$ and a wider temperature range data for $CuInS_2$.[30] The comparisons presented in Figs. 5 and 6 show quite good agreements between calculations and experiments, especially considering strongly indirect nature of the calculation procedure. For $CuInS_2$, the agreement is good

TABLE I. Comparison of calculated and experimental anisotropic temperature factors β_{ij} of $AgGaS_2$, $CuInS_2$, and $CuInSe_2$ at 298 K.

Atom	β_{11}	β_{22}	β_{33}	β_{23}	Reference
			$AgGaS_2$		
Ag	0.01290	β_{11}	0.00490	0	This work
Ag	0.01567	β_{11}	0.00567	0	Ref. 38
Ga	0.00650	β_{11}	0.00204	0	This work
Ga	0.00659	β_{11}	0.00193	0	Ref. 38
S	0.00670	0.00715	0.00266	0.00133	This work
S	0.00658	0.00762	0.00287	0.00171	Ref. 38
			$CuInS_2$		
Cu	0.01164	β_{11}	0.00257	0	This work
Cu	0.01315	β_{11}	0.00317	0	Ref. 39
In	0.00693	β_{11}	0.00170	0	This work
In	0.00851	β_{11}	0.00198	0	Ref. 39
S	0.00681	0.00681	0.00169	0.0002	This work
S	0.00918	0.00694	0.00210	−0.0019	Ref. 39
			$CuInSe_2$		
Cu	0.01061	β_{11}	0.00234	0	This work
Cu	0.01290	β_{11}	0.00357	0	Ref. 40
Cu	0.01229	β_{11}	0.00302	0	Ref. 41
In	0.00760	β_{11}	0.00178	0	This work
In	0.00767	β_{11}	0.00204	0	Ref. 40
In	0.00823	β_{11}	0.00201	0	Ref. 41
Se	0.00556	0.00682	0.00178	0.00002	This work
Se	0.00650	0.00768	0.00198	−0.0004	Ref. 40
Se	0.00623	0.00733	0.00251	0.00042	Ref. 41

TABLE II. Calculated anisotropic temperature factors β_{ij} of $AgGaSe_2$, $AgGaTe_2$, and $ZnSnP_2$ at 298 K.

Compound	Atom	β_{11}	β_{22}	β_{33}	β_{23}
$AgGaSe_2$	Ag	0.01572	β_{11}	0.00466	0
	Ga	0.00747	β_{11}	0.00212	0
	Se	0.00758	0.00827	0.00293	0.00167
$AgGaTe_2$	Ag	0.01366	β_{11}	0.00351	0
	Ga	0.01088	β_{11}	0.00173	0
	Te	0.01028	0.00961	0.00221	0.00006
$ZnSnP_2$	Zn	0.00633	β_{11}	0.00158	0
	Sn	0.00478	β_{11}	0.00138	0
	P	0.00511	0.00568	0.00131	−0.00015

in the low-temperatures range below 80 K (Fig. 6). With increasing temperature, the difference between calculation and experiment gradually increases to $T \approx 200$ K where the approximation is not expected to work very well and various other effects, which may probably include anharmonicity and defect formation, start to play important role. This is the same range of temperatures ($T \approx 200$ K) where we observe a divergence in the heat capacity (Fig. 1).

B. Temperature factors

The partial and total density of states were used to calculate, in the harmonic approximation, the atomic mean-square displacement matrix. In the ideal defect-free crystal, they describe the attenuation of x-ray or neutron-diffraction intensities due to the thermal oscillations of the atoms around their equilibrium positions, although usually they are modified by point defects contamination, other types of structural defects, or deviations from stoichiometry.[37] For comparison with experiment, the calculated mean-square displacement matrix elements were converted into the various temperature factors reported in the literature. Our results for $AgGaS_2$, $CuInS_2$, and $CuInSe_2$ anisotropic temperature factors β_{ij} at 298 K are compared in Table I with available experimental data.[38–41] Agreement between theory and experiment seems to be reasonable.

For completeness, we display in Table II the calculated anisotropic temperature factors of $AgGaSe_2$, $AgGaTe_2$, and $ZnSnP_2$ for which we did not find any experimental data.

Chalcopyrites are known for their anisotropic properties. Indeed, presented anisotropic temperature factors and previously calculated[3] elastic stiffness tensors and compressibilities point out on significant differences between properties

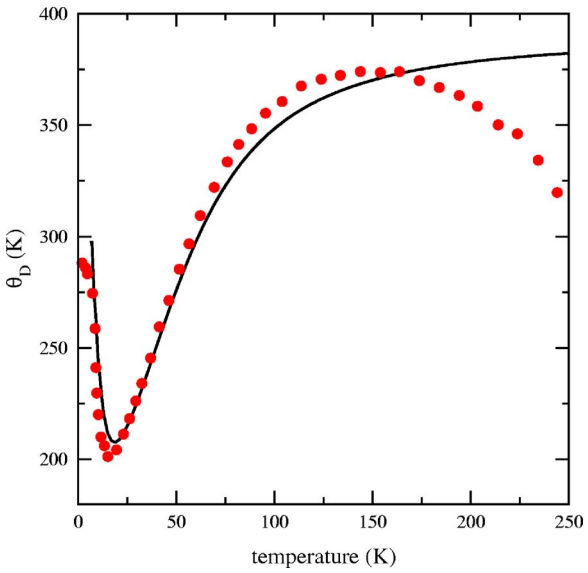

FIG. 6. (Color online) Temperature dependence of elastic Debye temperature of $CuInS_2$. Experimental data (filled circles) are taken from Ref. 30.

TABLE III. Comparison of calculated and experimental isotropic temperature factors $B(\mu)$ (all in $Å^2$) at 298 K.

Compound $A^{I}B^{III}C_2^{VI}$	B			Reference
	A^{I}	B^{III}	C^{VI}	
$AgGaS_2$	1.78	0.86	0.98	This work
	2.16	0.84	0.98	Ref. 38
$CuInS_2$	1.37	0.84	0.79	This work
	1.60	1.02	1.02	Ref. 39
	1.57	1.08	0.95	Ref. 44
$CuInSe_2$	1.36	1.00	0.87	This work
	1.79	1.05	0.99	Ref. 40
	1.65	0.62	0.72	Ref. 43
	1.65	2.87	1.23	Ref. 10
	1.26	3.01	0.77	Ref. 10
	1.33	2.28	1.46	Ref. 10
$AgGaSe_2$	2.23	1.04	1.22	This work
$AgGaTe_2$	2.12	1.48	1.47	This work
$ZnSnP_2$	0.68	0.83	0.64	This work

along and perpendicular to the longer lattice constant. However, sometimes[42] it is useful to know the isotropic temperature factors as well, which is just an orientational average of $B_{ij}(\mu)$. In Table III we add these values and compare them with the experimental data taken from literature. One can see overall good agreement. However, for $CuInSe_2$ the biggest discrepancy observed in B_{In} exceeds 100%. It is sightworthy that results reported by Zahn and Paufler[10] were obtained for Cu-poor samples with different concentrations of Cu vacancies, varying from 5.3% to 7.7%. We believe that observed differences between Zahn and Paufler data and our *ab initio* results as well as others experimental values are connected with nonstoichiometry causing well-known pair defects $V_{Cu}+2In_{Cu}$ which can enhance isotropic temperature factor of indium. On the other hand, any simple dependence of B on defect concentration cannot be derived.

IV. CONCLUSIONS

We have calculated the heat capacities at constant volumes, the elastic Debye's temperatures, and anisotropy temperature factors for a series of chalcopyrite compounds using the *ab initio* approach. The calculation results agree fairly well with available experimental data. Judging from the heat capacity results, the harmonic approximation works very well up to temperature $T\approx 200$ K, and for the case of $AgGaS_2$ this limit is even moved to higher value of $T\approx 400$ K. The elastic Debye temperature results are in good agreement with available data in the low-temperature range ($\leqslant 200$ K) further confirming that this is the range where the harmonic approximation works well. We expect that the results quoted in this paper for other compounds are also reliable and can serve as a guideline for future experimental works.

ACKNOWLEDGMENTS

The authors thank Susan Schorr for fruitful discussions and critical reading of the paper. The authors would like to express special thanks to Ingolf Neumann and Andreas Neumann, the sons of the late Hans Neumann, for kind help in collecting experimental data for this paper after the death of their father. This work was partially supported by Marie Curie Research Training Network under Contract No. MRTN-CT-2006-035957 (c2c). J.Ł. acknowledges support by the Polish Ministry of Science and Education under Project No. 1 P03B 104 26. Calculations have been partially performed in the Interdisciplinary Center for Mathematical and Computational Modeling at Warsaw University.

*Corresponding author. Electronic address: jan.lazewski@ifj.edu.pl

[1] F. W. Ohrendorf and H. Haeuseler, Cryst. Res. Technol. **34**, 339 (1999).
[2] J. Łażewski, H. Neumann, K. Parlinski, G. Lippold, and B. J. Stanbery, Phys. Rev. B **68**, 144108 (2003).
[3] J. Łażewski, H. Neumann, P. T. Jochym, and K. Parlinski, J. Appl. Phys. **93**, 3789 (2003).
[4] M. Blackman, *Encyclopedia of Physics*, Edited by S. Flügge (Springer-Verlag, Berlin, 1955), Vol. VII/I, p. 325.
[5] N.-H. Kim, D. H. Shin, and R. S. Feigelson, Mater. Sci. Eng., B **38**, 229 (1996).
[6] O. Brisson, A. Simonnet, B. Darriet, and J.-C. Launay, J. Cryst. Growth **193**, 597 (1998).
[7] H. Neumann and E. Nowak, J. Less-Common Met. **146**, L7 (1989).
[8] O. Brisson, M. El Ganaoui, A. Simonnnet, and J.-C. Launay, J. Cryst. Growth **204**, 201 (1999).
[9] H. Neumann, G. Kühn, and W. Möller, Cryst. Res. Technol. **20**, 1225 (1985).
[10] G. Zahn and P. Paufler, Cryst. Res. Technol. **23**, 499 (1988).
[11] J. M. Merino, J. L. Martin de Vidales, S. Mahanty, R. Diaz, F. Rueda, and M. Leon, J. Appl. Phys. **80**, 5610 (1996).
[12] J. Łażewski and K. Parlinski, J. Chem. Phys. **114**, 6734 (2001).
[13] J. Łażewski, P. T. Jochym, and K. Parlinski, J. Chem. Phys. **117**, 2726 (2002).
[14] J. Łażewski, K. Parlinski, B. Hennion, and R. Fouret, J. Phys.: Condens. Matter **11**, 9665 (1999).
[15] J. Łażewski and K. Parlinski, J. Phys.: Condens. Matter **11**, 9673 (1999).
[16] G. Kresse and J. Furthmüller, VASP software, Vienna, 1999; Phys. Rev. B **54**, 11169 (1996); Comput. Mater. Sci. **6**, 15 (1996).
[17] P. E. Blöchl, Phys. Rev. B **50**, 17953 (1996).
[18] G. Kresse and D. Joubert, Phys. Rev. B **59**, 1758 (1999).
[19] J. P. Perdew and A. Zunger, Phys. Rev. B **23**, 5048 (1981).
[20] J. P. Perdew, J. A. Chevary, S. H. Vosko, K. A. Jackson, M. R. Pederson, D. J. Singh, and C. Fiolhais, Phys. Rev. B **46**, 6671 (1992).
[21] H. J. Monkhorst and J. D. Pack, Phys. Rev. B **13**, 5188 (1976).
[22] K. Parlinski, Z. Q. Li, and Y. Kawazoe, Phys. Rev. Lett. **78**, 4063 (1997).
[23] K. Parlinski, PHONON software, 2005.
[24] G. H. Golub and C. F. Van Loan, *Matrix Computations*, 3rd ed. (Johns Hopkins University Press, Baltimore, 1996).
[25] W. Koschel and M. Bettini, Phys. Status Solidi B **72**, 729 (1975).
[26] H. Neumann, W. Kissinger, H. Sobotta, V. Riede, R. D. Tomlinson, and N. Avgerinos, Czech. J. Phys., Sect. B **34**, 69 (1984).
[27] N. V. Joshi, J. Raman Spectrosc. **11**, 517 (1981).
[28] K. Wakita, H. Hirooka, S. Yasuda, F. Fujita, and N. Yamamoto, J. Appl. Phys. **83**, 443 (1998).
[29] J. J. M. Binsma, L. J. Giling, and J. Bloem, J. Cryst. Growth **50**, 429 (1980).
[30] K. J. Bachmann, F. S. L. Hsu, F. A. Thiel, and H. M. Kasper, J. Electron. Mater. **6**, 431 (1977).
[31] H. Neumann, G. Kühn, and W. Möller, Phys. Status Solidi B **144**, 565 (1987).
[32] I. V. Bodnar, Inorg. Mater. **36**, 108 (2000).
[33] I. V. Bodnar and N. S. Orlova, Izv. Akad. Nauk SSSR, Neorg. Mater. **25**, 382 (1989).
[34] P. Derollez, J. Gonzalez, B. Hennion, and R. Fouret, Physica B **305**, 191 (2001).

[35] S. C. Abrahams and F. S. L. Hsu, J. Chem. Phys. **63**, 1162 (1975).
[36] P. A. Varotsos, Phys. Status Solidi A **49**, K57 (1978).
[37] D. L. Price, M.-L. Saboungi, and F. J. Bermejo, Rep. Prog. Phys. **66**, 407 (2003).
[38] S. C. Abrahams and J. L. Bernstein, J. Chem. Phys. **59**, 1625 (1973).
[39] S. C. Abrahams and J. L. Bernstein, J. Chem. Phys. **59**, 5415 (1973).
[40] K. S. Knight, Mater. Res. Bull. **27**, 161 (1992).
[41] K. Nagata, Y. Miyamoto, and K. Takarabe, Fukuoka Daigaku Rigaku Shuho **19**, 103 (1989).
[42] W. C. Hamilton, Acta Crystallogr. **12**, 609 (1959).
[43] M. Kh. Rabadanov and I. A. Verin, Inorg. Mater. **34**, 14 (1998).
[44] N. Avgerinos, Ph.D. thesis, University Salford, 1983.